LTR-PAFM-08-4 Rev. 0

Technical Basis to Support Extension of Surveillance Interval For Planned Visual Inspection of the Indian Point Unit 2 BMI Nozzles

January 2008

Author: C. K. Ng*
Piping Analysis and Fracture Mechanics

Verifier: A. Udyawar*
Piping Analysis and Fracture Mechanics

Approved: S. A. Swamy*
Manager, Piping Analysis and Fracture Mechanics

Electronically approved records are authenticated in the electronic document management system.

Westinghouse Electric Company LLC
P.O. Box 355
Pittsburgh, PA 15230-0355

1.0 INTRODUCTION

The purpose of this report is to provide a technical basis to support a longer visual inspection interval of the Bottom Mounted Instrumentation (BMI) nozzles at Indian Point Unit 2. Since the BMI penetration nozzle configurations and geometries for both Indian Point Units 2 and 3 are quite similar, the results and conclusions provided in this letter report are also applicable to Indian Point Unit 3, if such a technical basis is needed for Unit 3, provided the Unit 3 bottom head operating temperature is the same as Unit 2.

The Indian Point Unit 2 BMI penetration nozzles were inspected by NDE (Non Destructive Examination) from the reactor vessel inside surface during the R17 outage in April 2006. During that outage, no indications were detected in the BMI penetration nozzles. In order to be able to extend the visual inspection surveillance interval, the following key issues must be addressed:

- What is the maximum undetected flaw size based on the current NDE detection capability for the BMI penetration nozzles?
- How long does it take for such undetected flaw to grow through-wall and result in leakage of a BMI penetration nozzle?
- How large a flaw would be required to result in failure of a BMI penetration nozzle?

A structural integrity evaluation of the BMI penetration nozzles is necessary to address the above issues. Finite element stress analyses were carried out using the ANSYS program and the stress analysis results were used as input to the structural integrity evaluation. The results of the structural integrity evaluation were then used to develop the required technical basis. A discussion of the finite element stress analyses and the structural integrity evaluation performed are provided in Sections 2.0 and 3.0 respectively.

2.0 FINITE ELEMENT STRESS ANALYSIS

The objective of the finite element stress analysis was to obtain the steady state condition stresses in the BMI penetration nozzles. These stresses are one of the input parameters required in the structural integrity evaluation. Three dimensional elastic plastic finite element analyses were performed for the BMI penetration nozzle configurations and geometries of Indian Point Unit 2 (Reference 1) and Unit 3 (Reference 2). The BMI penetration nozzle geometries for both units (References 3 and 4) are summarized in Table 2-1. Four BMI penetration nozzles for each unit were analyzed and the results were used to provide representative results for the remaining unanalyzed nozzles located on the bottom of the reactor vessel head.

Table 2-1

Indian Point Units 2 and 3 Nozzle Geometries

BMI Nozzle	Outside Diameter (inches)	Inside Diameter (inches)	Thickness (inches)
Unit 2	1.499	0.460	0.520
Unit 3	1.499	0.507	0.496

2.1 Model

Three-dimensional finite element model comprised of iso-parametric brick and wedge elements was used to obtain the steady state condition hoop and axial stresses. A sketch for a typical BMI nozzle finite element model is shown in Figure 2-1. Taking advantage of the symmetry of the vessel bottom head, only half of a BMI penetration nozzle was modeled. In the model, the upper portion of the BMI penetration nozzle, adjacent section of the vessel bottom head and the joining weld were modeled. The vessel to penetration nozzle weld was simulated with four weld passes. The penetration nozzle, weld metal, cladding and the vessel bottom head shell were modeled in accordance with the relevant material properties.

The only loads used in the analysis are the steady state operating loads. External loads, such as seismic loads, have been studied and have negligible impact since the penetration nozzles are captured by the full thickness of the reactor vessel bottom head with only minimal gaps. In addition, the duration of the seismic loading is very short and will not have any significant impact on the overall Primary Water Stress Corrosion Crack (PWSCC) growth. The area of interest is in the BMI penetration nozzle near the attachment weld, which is not significantly affected by these external loads.

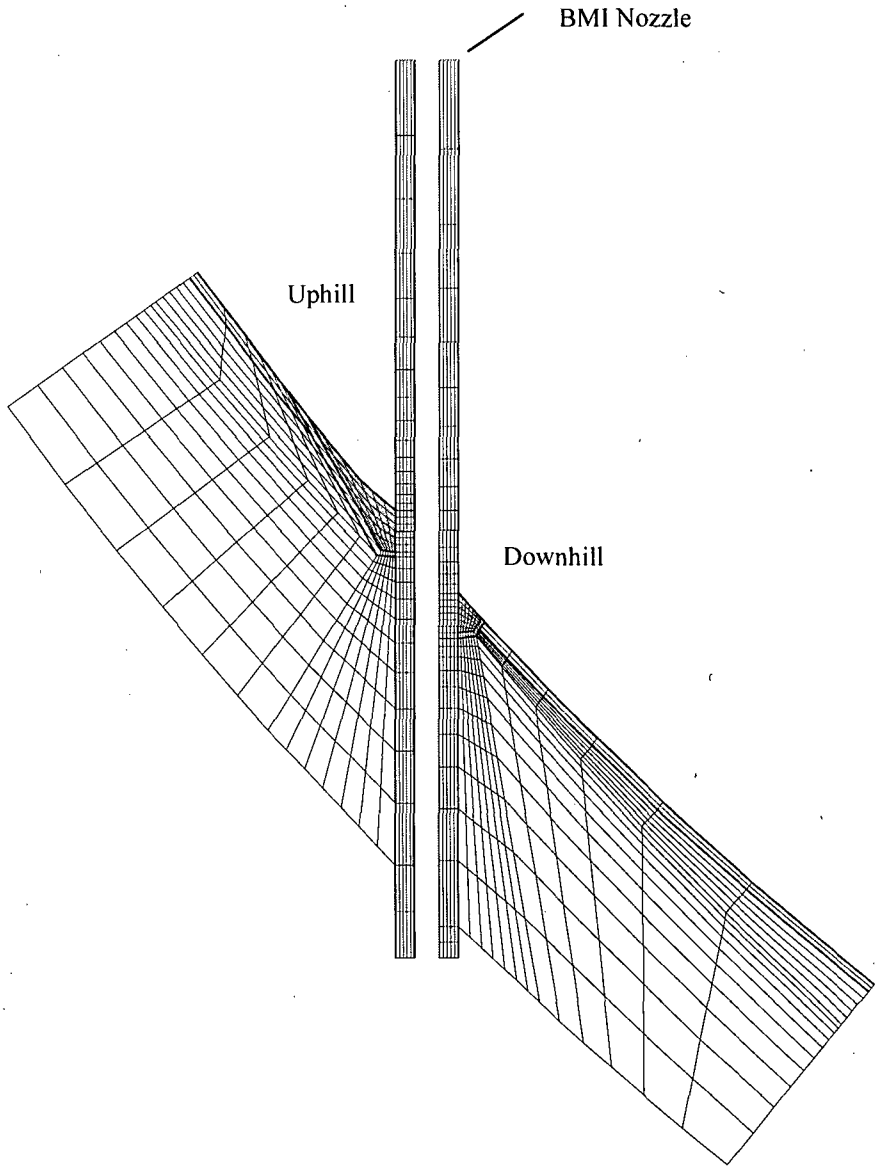

Figure 2-1 Typical BMI Penetration Nozzle Finite Element Model

2.2 Stress Analysis Results

There are no significant differences in the stress results between Indian Point Units 2 and 3 because the BMI penetration nozzle configurations and geometries for both units are quite similar and the same bottom head temperature of 537 °F was used for both units. Figures 2-2 through 2-5 presents the typical hoop and axial stress contours under the steady state condition for four BMI penetration nozzles. The stress contours in Figures 2-2 through 2-5 represent those for the Indian Point Unit 2 BMI penetration nozzles and the corresponding stress contours for Unit 3 are similar.

The hoop stresses under steady state condition are much higher than the axial stresses. This is consistent with the stress analysis results from the reactor vessel upper head penetration nozzles. Typically, in-service cracks will orient themselves perpendicular to the largest stress component and the cracks discovered in the upper head penetration nozzles are generally oriented axially. Also it should be noted that the highest stresses are found at the uphill side and downhill side locations rather than midway around the penetration nozzle. This is consistent with finding axial cracks typically in the vicinity of the uphill side and downhill side locations. It is these steady state stresses that will be used to predict PWSCC crack growth in the BMI penetration nozzles.

The stress results also support the safety argument that cracks are unlikely to propagate in the circumferential direction because the axial stresses are relatively low and there is a small area of compressive axial stress in the BMI penetration nozzles. This is illustrated in a cut taken along the plane on the bottom of the attachment weld of the Indian Point Unit 2 BMI penetration nozzles, as shown in Figures 2-6 through 2-9. Similar observations can be made for the Indian Point Unit 3 BMI penetration nozzles.

The stress analysis results from the four analyzed nozzles (5.5°- centermost, 20.2°, 34.0°, and 48.5°- outermost) were used to represent those for the remaining unanalyzed BMI penetration nozzles in the reactor vessel bottom head. It should be noted that bounding stress results from both Indian Point Units 2 and 3 were used as input to the structural integrity evaluation discussed in Section 3.0.

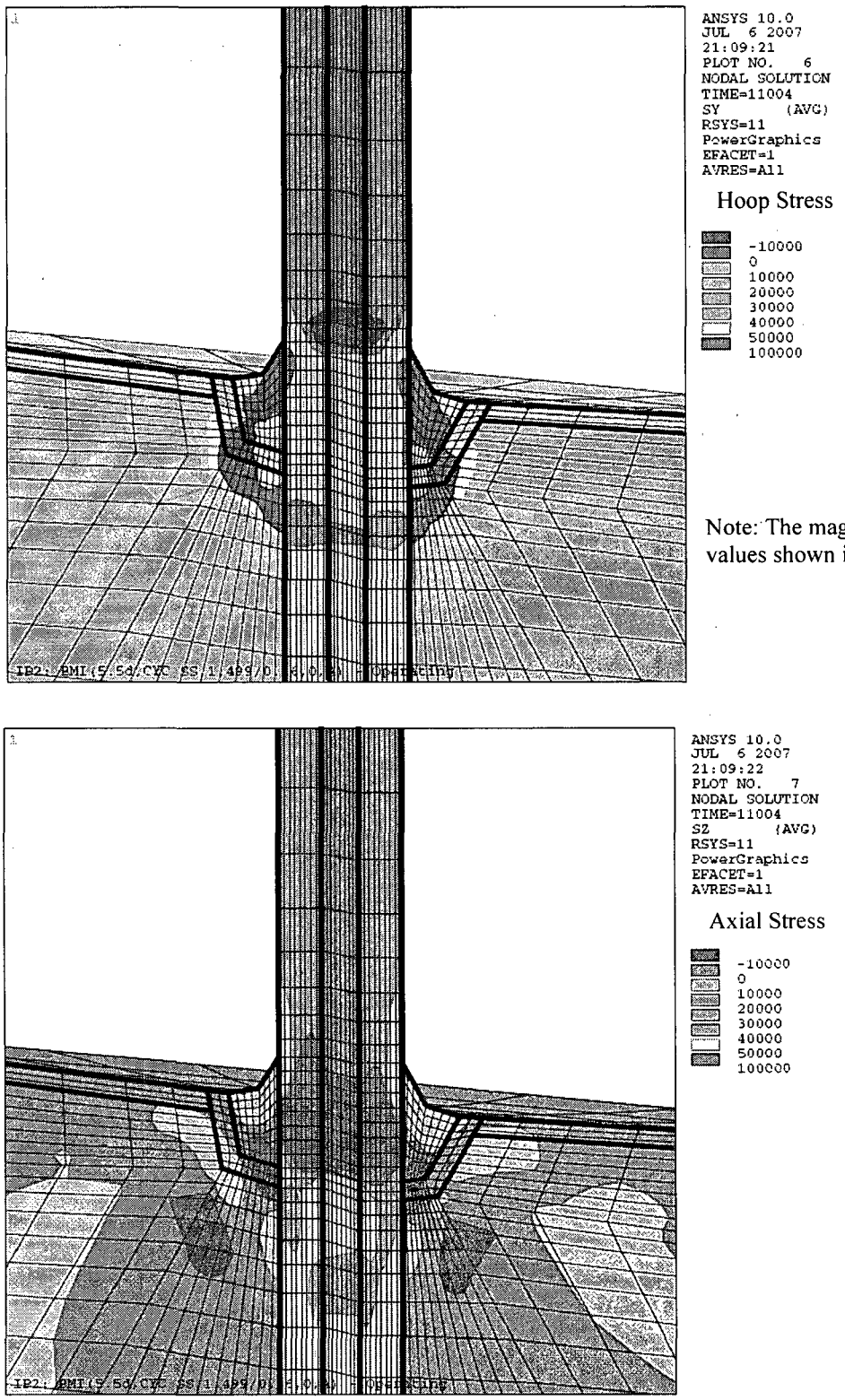

Note: The magnitude of the stress values shown is in psi

Figure 2-2
Hoop and Axial Stress Distribution at Steady State Conditions for Unit 2 BMI Penetration (5.5°)

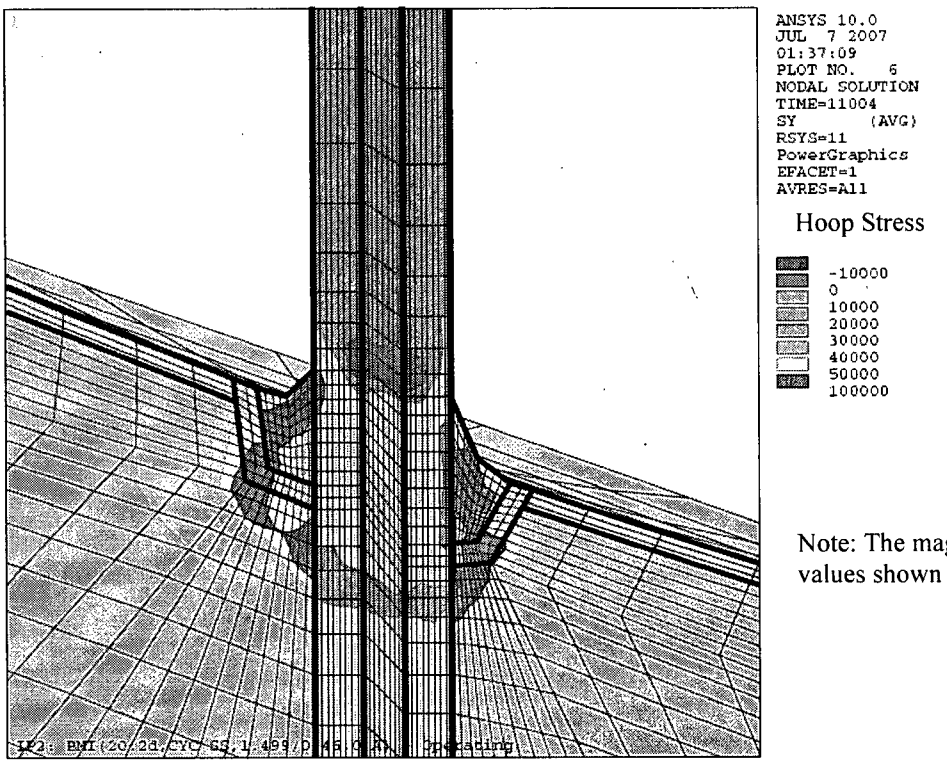

Note: The magnitude of the stress values shown is in psi

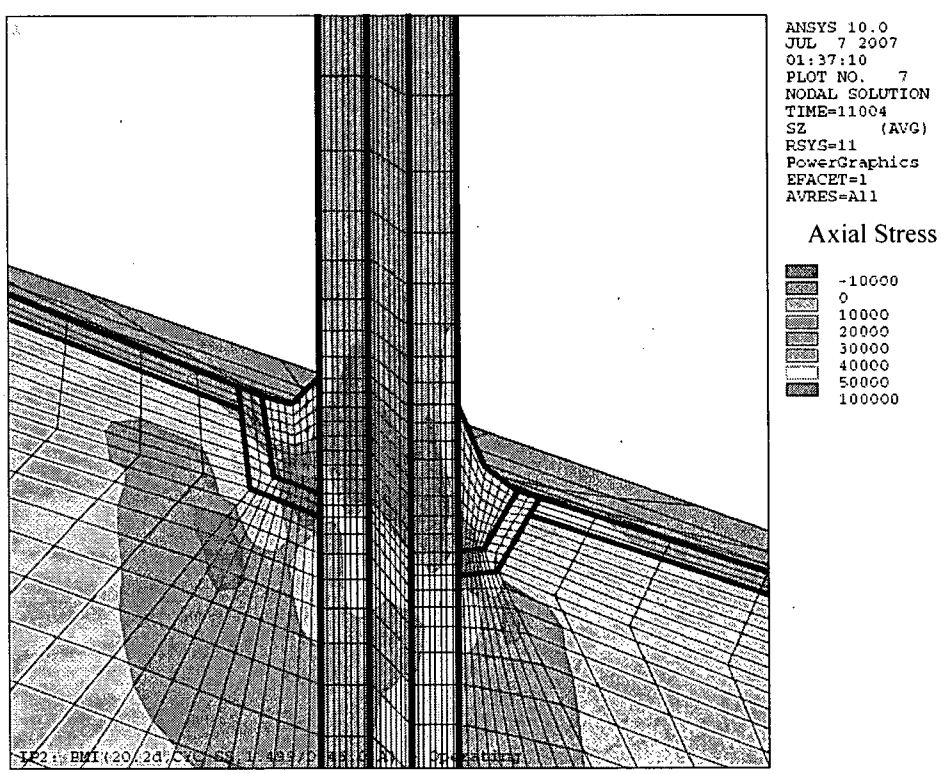

Figure 2-3
Hoop and Axial Stress Distribution at Steady State Conditions for Unit 2 BMI Penetration (20.2°)

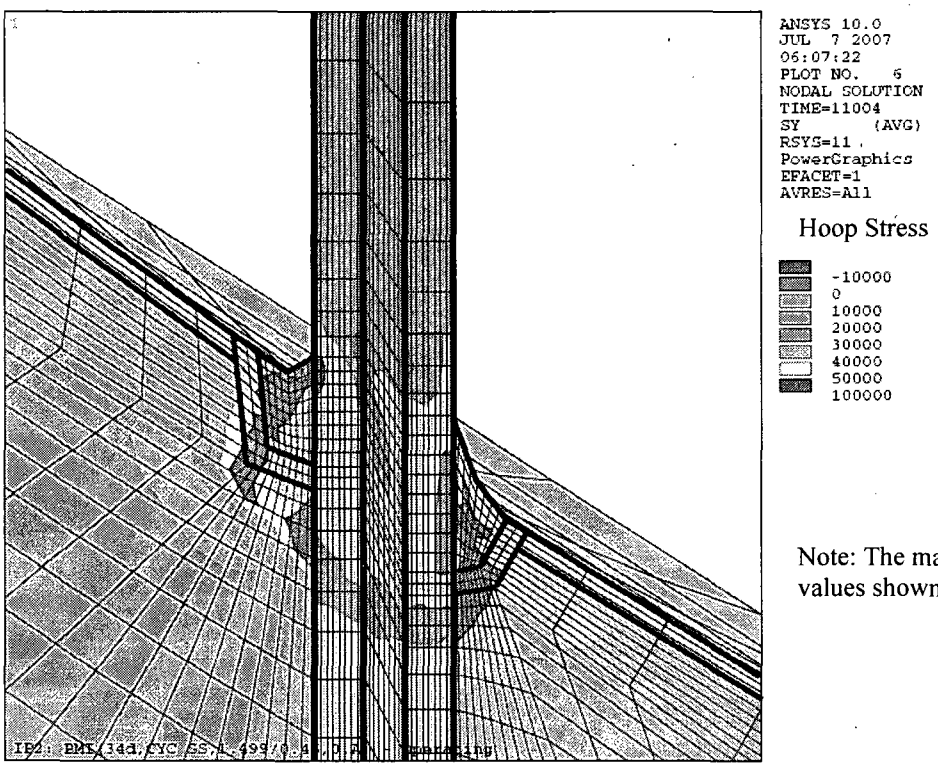

Note: The magnitude of the stress values shown is in psi

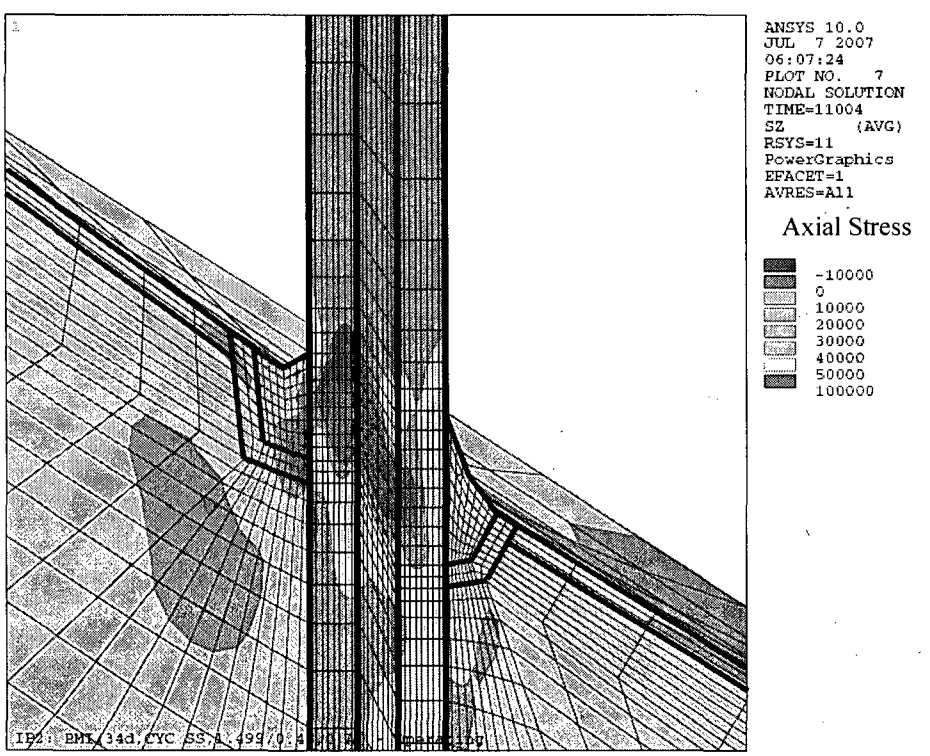

Figure 2-4
Hoop and Axial Stress Distribution at Steady State Conditions for Unit 2 BMI Penetration (34.0°)

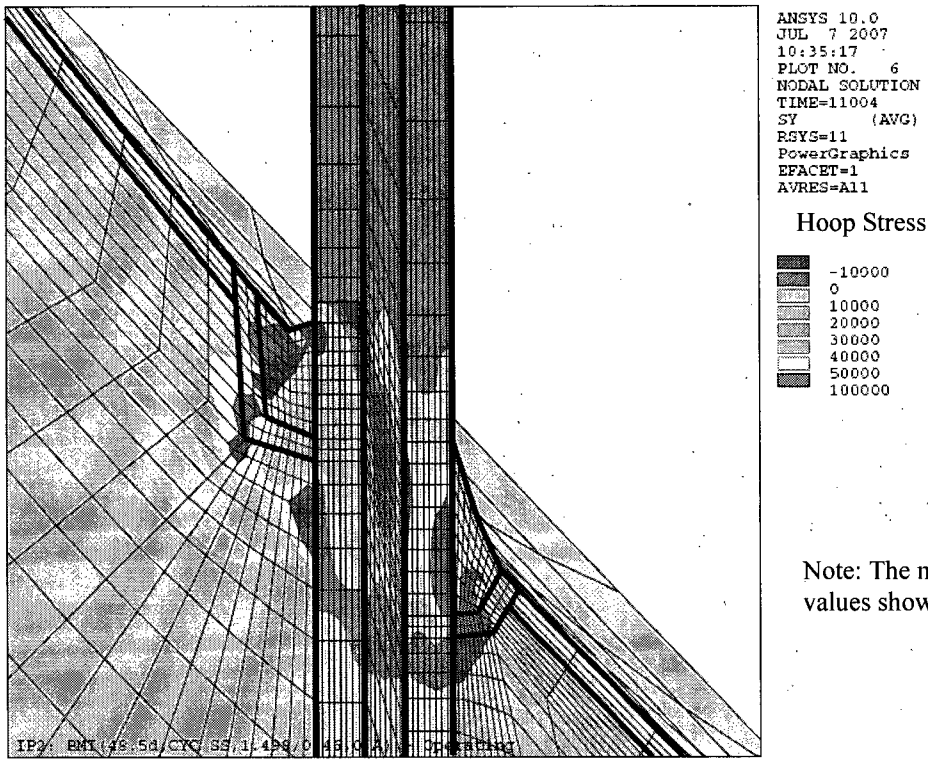

Note: The magnitude of the stress values shown is in psi

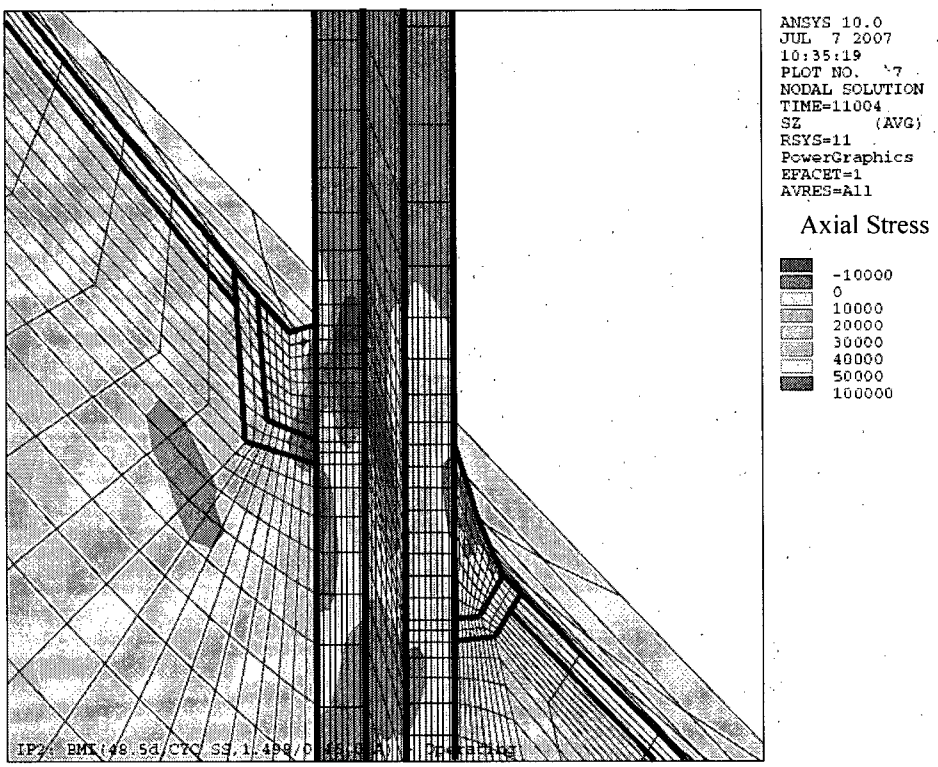

Figure 2-5
Hoop and Axial Stress Distribution at Steady State Conditions for Unit 2 BMI Penetration (48.5°)

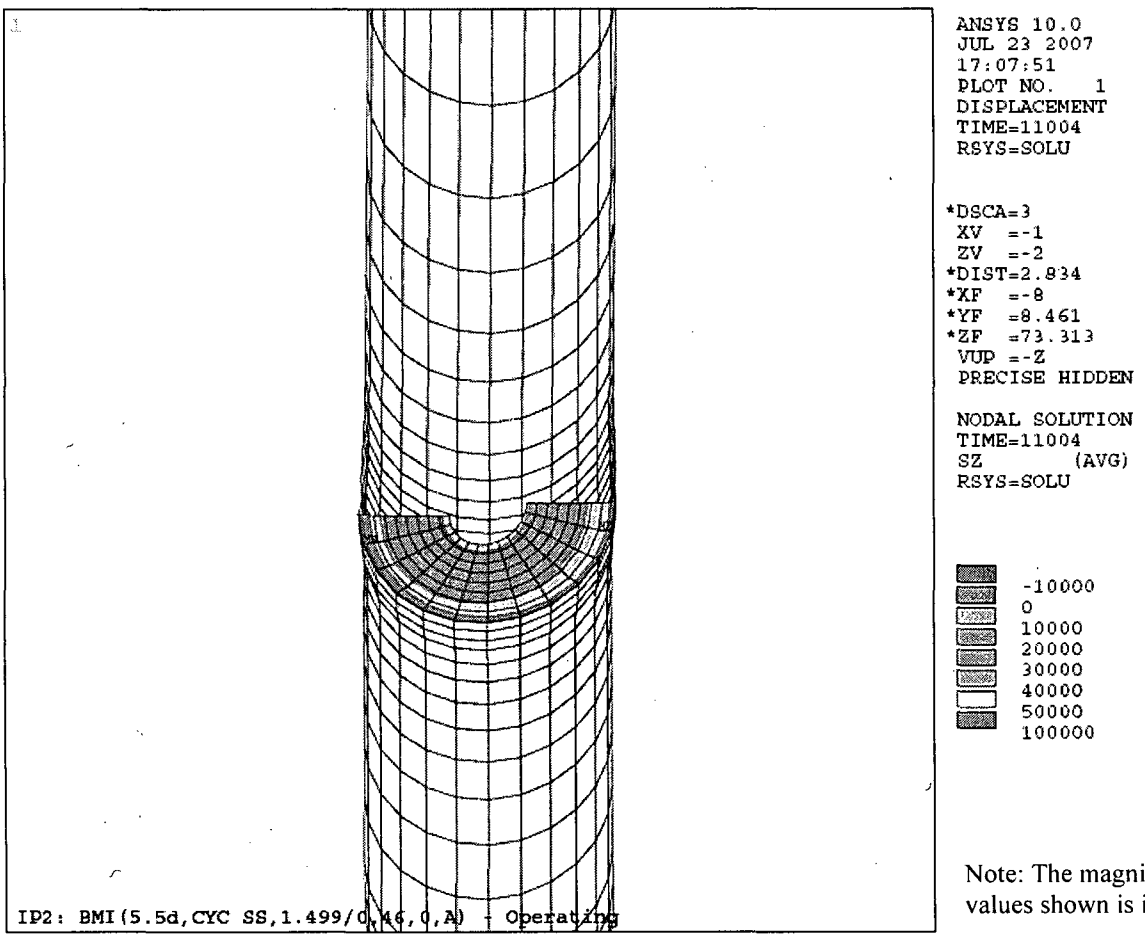

Note: The magnitude of the stress values shown is in psi

Figure 2-6

Axial Stress Distribution at Steady State Conditions for the Unit 2 BMI Penetration (5.5°) along a Plane Oriented Parallel to, and Just Below the Attachment Weld

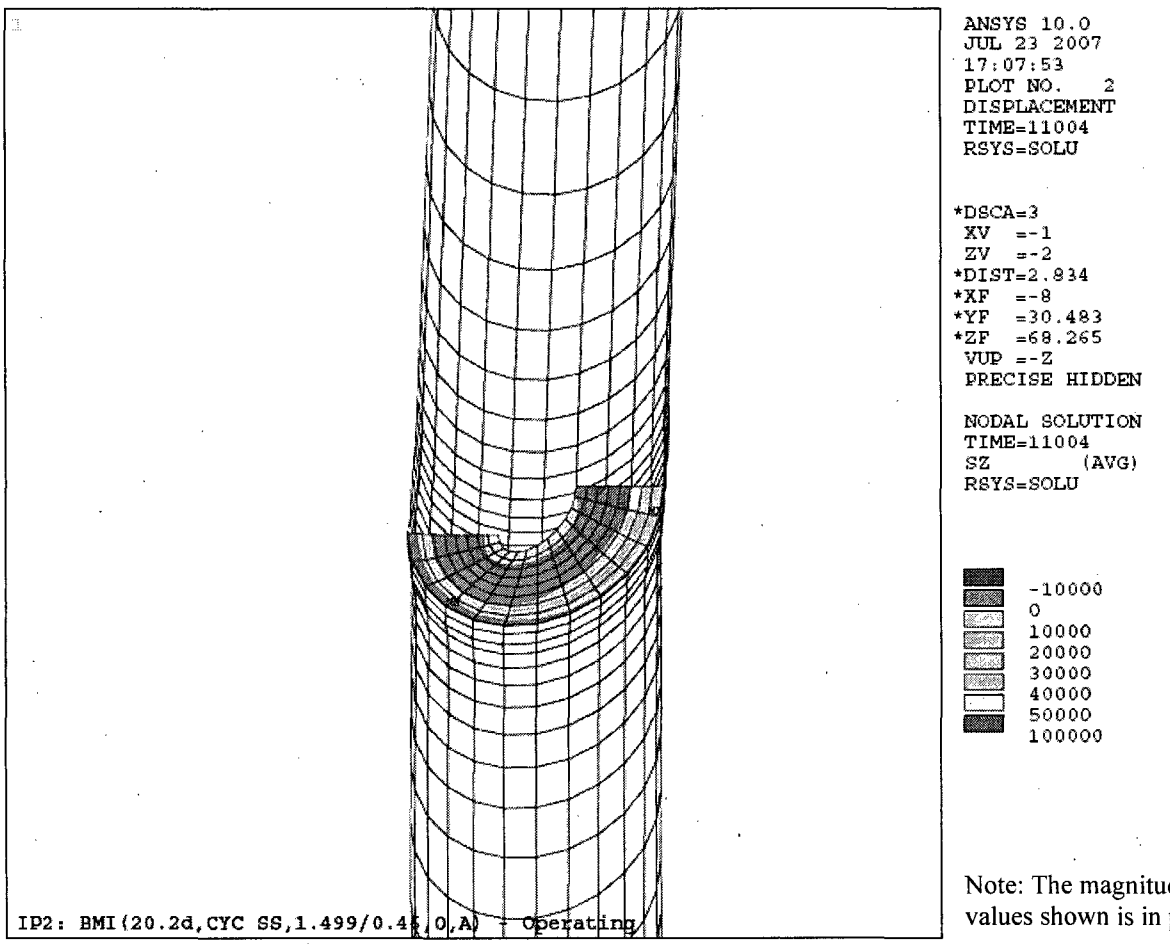

Note: The magnitude of the stress values shown is in psi

Figure 2-7

Axial Stress Distribution at Steady State Conditions for the Unit 2 BMI Penetration (20.2°) along a Plane Oriented Parallel to, and Just Below the Attachment Weld

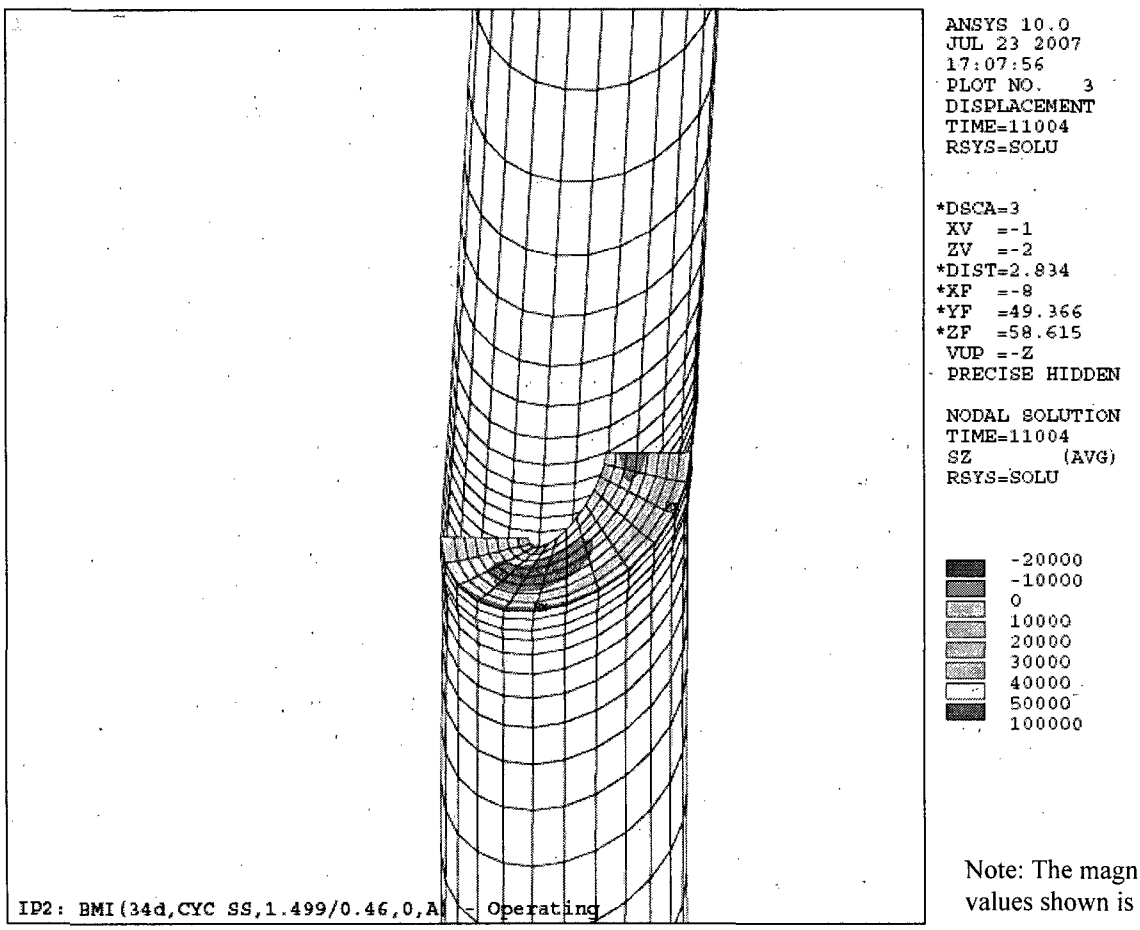

Note: The magnitude of the stress values shown is in psi

Figure 2-8

Axial Stress Distribution at Steady State Conditions for the Unit 2 BMI Penetration (34.0°) along a Plane Oriented Parallel to, and Just Below the Attachment Weld

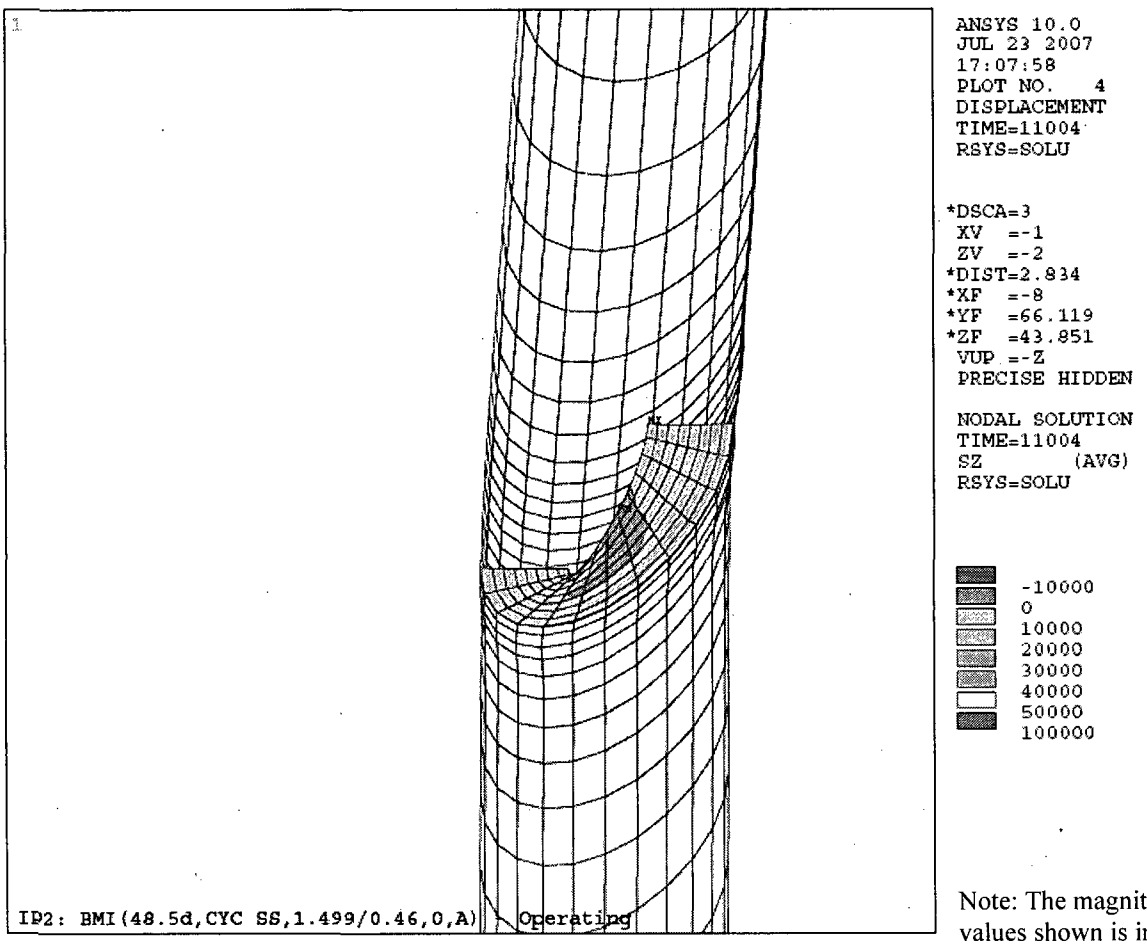

Note: The magnitude of the stress values shown is in psi

Figure 2-9

Axial Stress Distribution at Steady State Conditions for the Unit 2 BMI Penetration (48.5°) along a Plane Oriented Parallel to, and Just Below the Attachment Weld

3.0 STRUCTURAL INTEGRITY EVALUATION

3.1 Introduction

The Indian Point Unit 2 BMI penetration nozzles have been inspected by NDE from the reactor vessel inside surface during the R17 outage in April 2006. During that outage, no indications were detected in the BMI penetration nozzles. In order to defer the visual inspection to the R20 outage in April 2012 and avoid doing visual inspections during the R18 and R19 outages, the following issues need to be addressed:

- What is the maximum undetected flaw size based on the current NDE detection capability for the BMI penetration nozzles?
- How long does it take for such undetected flaw to grow through the wall and result in leakage of a BMI penetration nozzle?
- How large a flaw would be required to result in failure of a BMI penetration nozzle?

These issues are addressed in the following sections.

3.2 NDE Detection Capability for BMI Penetration Nozzles

The maximum undetected flaw size based on the NDE detection capability during R17 outage for the BMI penetration nozzles is [ ] inch in depth and [ ] inch in length. The rationale for this recommendation is provided in Reference 5 and is attached in Appendix A of this letter report.

3.3 Crack Growth Evaluation

Initial Flaw Size

In order to determine the service life required for a given flaw size to grow through the wall and result in leakage, PWSCC crack growth evaluations were performed. Since the maximum undetected flaw size in the BMI penetration nozzle during the R17 outage is [ ] inch in depth and [ ] inch in length, it is conservative to assume an initial undetected flaw with a depth of 0.10 inch and an aspect ratio (length/depth) of 6 (i.e. flaw length = 0.60 inch) in the crack growth evaluation. Both axial and circumferential flaw orientations were considered.

PWSCC Growth Rate Curve

The Electric Power Research Institute - Materials Reliability Program (EPRI-MRP) crack growth review team, an international panel of experts in the area of Stress Corrosion Cracking (SCC) crack growth, provided input to the development of the recommended crack growth rate curve (Reference 6).

The recommended PWSCC growth rate curve for Alloy 600 material is as follows:

MRP recommends that this curve be applied to the growth evaluations of SCC flaws in Alloy 600 materials exposed to the primary water environment. The PWSCC growth rate model used for Indian Point Units 2 and 3 reactor vessel BMI nozzles for an operating temperature of 280.6 °C (537 °F) is:

$$\frac{da}{dt} = 3.28 \times 10^{-13} (K - 9)^{1.16} \text{ m/sec}$$

Stress Intensity Factor

Stress intensity factor is needed to determine the crack growth rate. The bounding stress distribution from both Indian Point Units 2 and 3 was used to calculate the stress intensity factor. The crack growth evaluation was performed by postulating both axial and circumferential flaws at the location with the worst stress distribution through the wall in the BMI penetration nozzles. The highest stress location was found to be in the immediate vicinity of the J-groove weld. The through-wall stress profile was represented by a cubic polynomial.

$$\sigma(x) = A_0 + A_1 x + A_2 x^2 + A_3 x^3$$

where :

x	=	coordinate distance into the nozzle wall
σ	=	stress perpendicular to the plane of the crack
A_i	=	coefficients of the cubic polynomial fit

For surface flaws with aspect ratio of 6, the stress intensity factor expression of Raju and Mettu (Reference 7) was used. The stress intensity factor K_I (Φ) was calculated at the point of maximum crack depth and is represented by $\Phi = 0$. The following expression was used for calculating K_I (Φ), where Φ is the angular location around the crack. The units of K_I (Φ) are in

$ksi\sqrt{in}$.

$$K_I(\Phi) = \left[\frac{\pi a}{Q}\right]^{0.5} \sum_{j=0}^{3} G_j\left(a/c,\ a/t,\ t/R,\ \Phi\right) A_j\, a^j$$

The boundary correction factors G_0 (Φ), G_1 (Φ), G_2 (Φ) and G_3 (Φ) were obtained from the procedure outlined in Reference 7. The dimension "a" is the crack depth, and "c" is the semi crack length, while "t" is the wall thickness. "R" is the inside radius of the tube, and "Q" is the shape factor.

Once the stress intensity factor has been determined, crack growth analysis of the postulated flaw in each of the four BMI penetration nozzles were performed. The flaw is assumed to be subjected to PWSCC based on the PWSCC crack growth rate for Alloy 600 material recommended in MRP-55 (Reference 6).

3.4 Crack Growth Charts

The results of the crack growth evaluation are presented in the form of simple crack growth charts. The charts graphically show the crack depth to wall thickness ratio as a function of service life in Effective Full Power Years (EFPY). Crack growth curves for each of the BMI penetration nozzle analyzed are included in the chart.

Crack growth curves generated for both inside and outside axial surface flaws for four BMI penetration nozzles are shown in Figures 3-1 and 3-2 respectively. Similar crack growth curves for both inside and outside circumferential surface flaws are shown in Figures 3-3 and 3-4 respectively. The crack growth charts are applicable to both Indian Point Units 2 and 3 since bounding stress results and nozzle geometries were used in the generation of the crack growth curves for the same bottom head normal operating temperature of 537°F.

The results of the crack growth analysis shown in Figures 3-1 and 3-2 were based on an initial flaw depth of 0.1 inch and a flaw length of 0.6 inch. This assumed initial flaw size is well within the current NDE detection capability of [ ] inch in flaw depth and [ ] inch in length. Based on this initial flaw depth (a/t=0.20, a = 0.1 inch and t = 0.496 in), the most limiting results shown in Figures 3-1 and 3-2 indicated that it would take at least 5.4 EFPY for an outside axial surface flaw to reach 75% of the nozzle wall thickness, which is more than two refueling cycles and through wall leakage is not expected to occur in less than 6 EFPY.

As discussed in Section 2.2, the hoop stresses under steady state condition are much higher than the axial stresses. As a result, using the same initial flaw size for circumferential flaws as used in determining the crack growth for axial flaws, the resulting stress intensity factor was found to be quite small and would not result in any meaningful crack growth. Therefore, larger initial flaw sizes were used to determine the crack growth for circumferential flaws as shown in Figures 3-3 and 3-4. The larger initial flaw depths were conservatively chosen such that the resulting stress intensity factor is 15 $MPa\sqrt{m}$ which exceeded the threshold value of 9 $MPa\sqrt{m}$. It should be noted that the circumferential crack growth results for BMI penetration nozzles with nozzle

angles of 5.5° and 20.2° are not shown in Figures 3-3 to 3-4 because the through-wall axial stresses for these nozzles are either compressive or too small to result in any meaningful crack growth even for larger initial flaw depths. The limiting result from both figures shows that leakage is not expected to occur in less than 20 EFPY even for large postulated initial flaw sizes well within the current NDE detection capability.

Based on the crack growth results shown in Figures 3-1 to 3-4, it can be concluded that axial outside surface flaw would result in the most limiting crack growth result. For an initial flaw depth of 0.10 inch and a flaw length of 0.60 inch, leakage is not expected to occur in less than 6 EFPY.

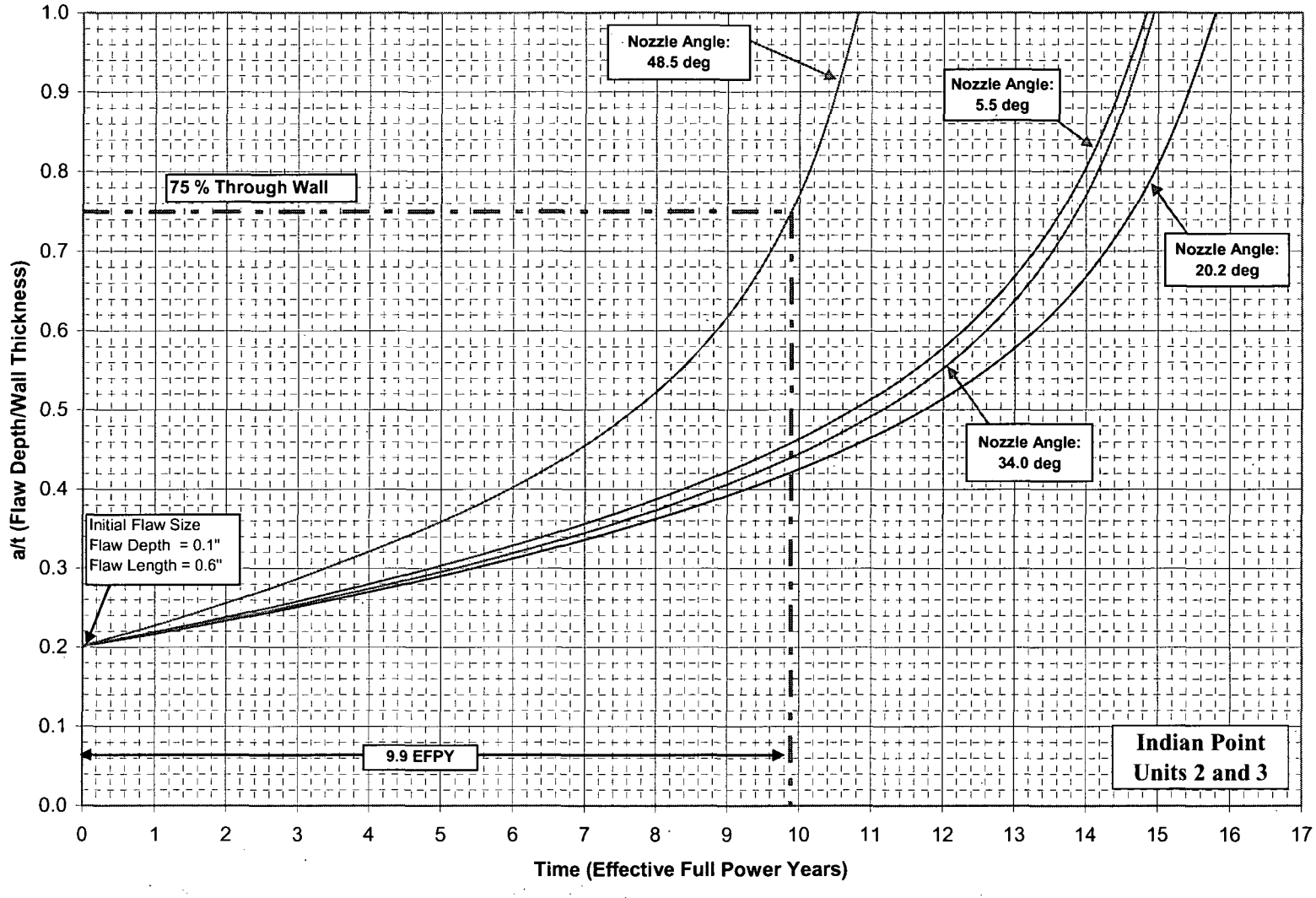

Figure 3-1 Crack Growth Results for Axial Inside Surface Flaws

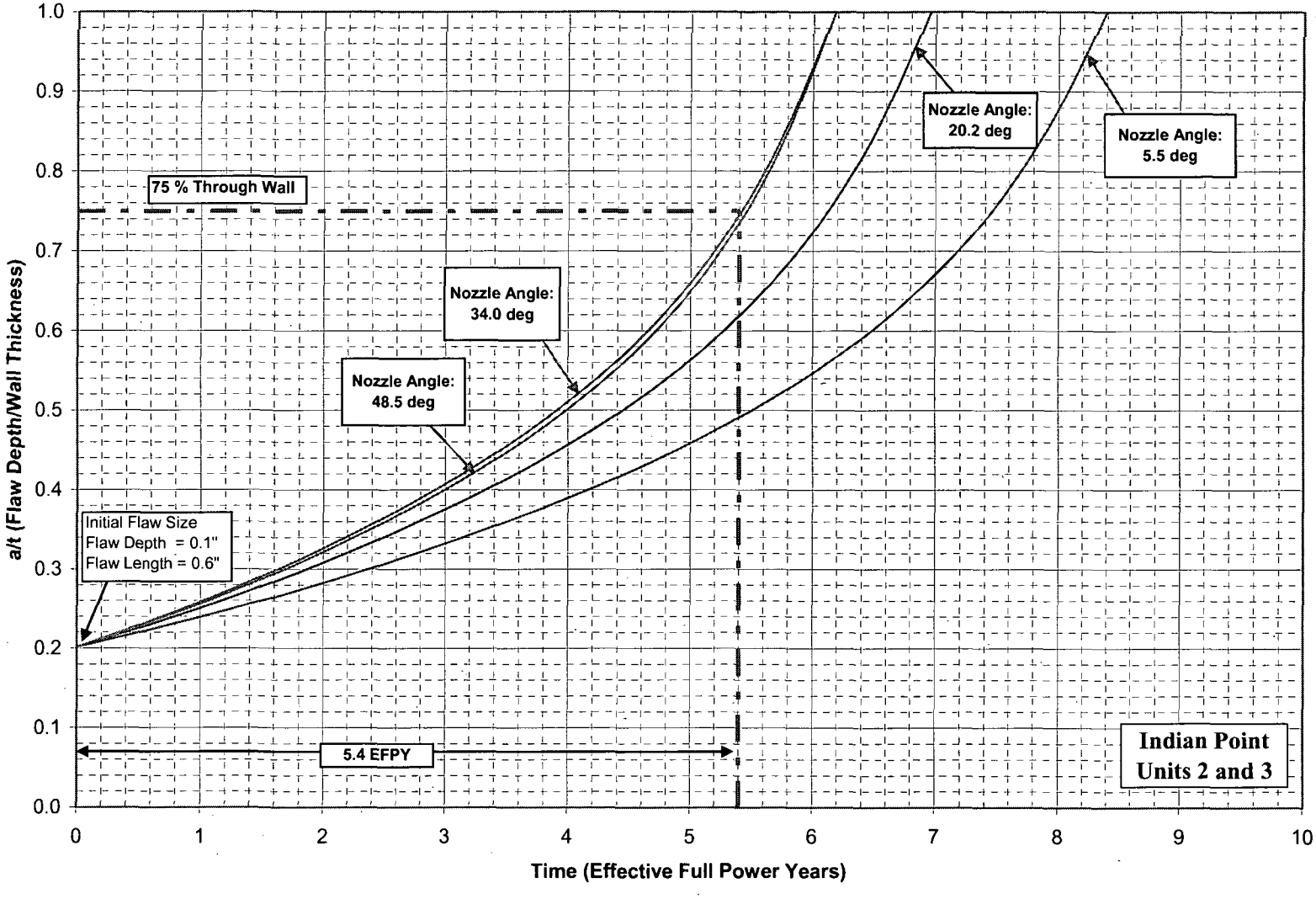

Figure 3-2 Crack Growth Results for Axial Outside Surface Flaws

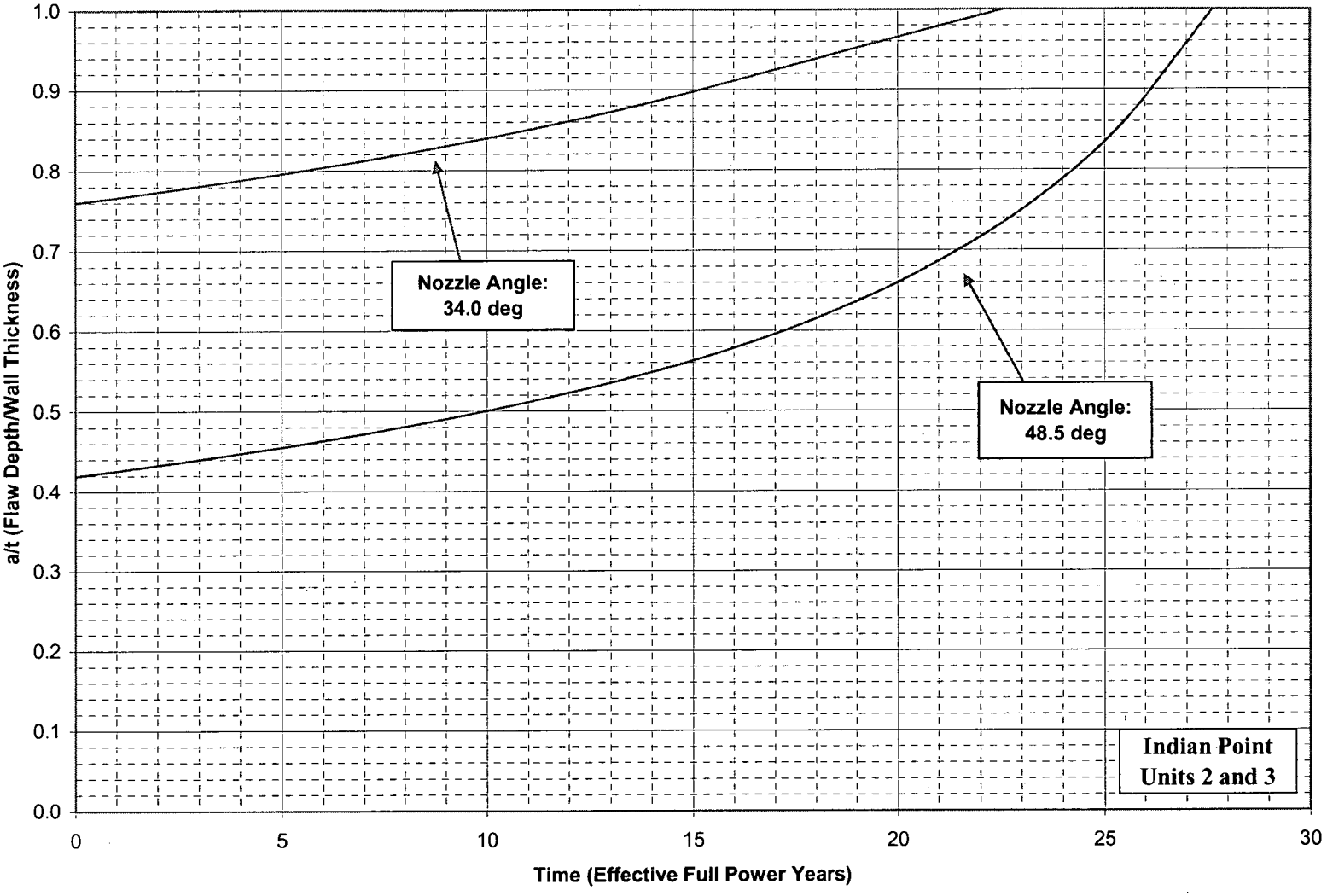

Figure 3-3 Crack Growth Results for Circumferential Inside Surface Flaws

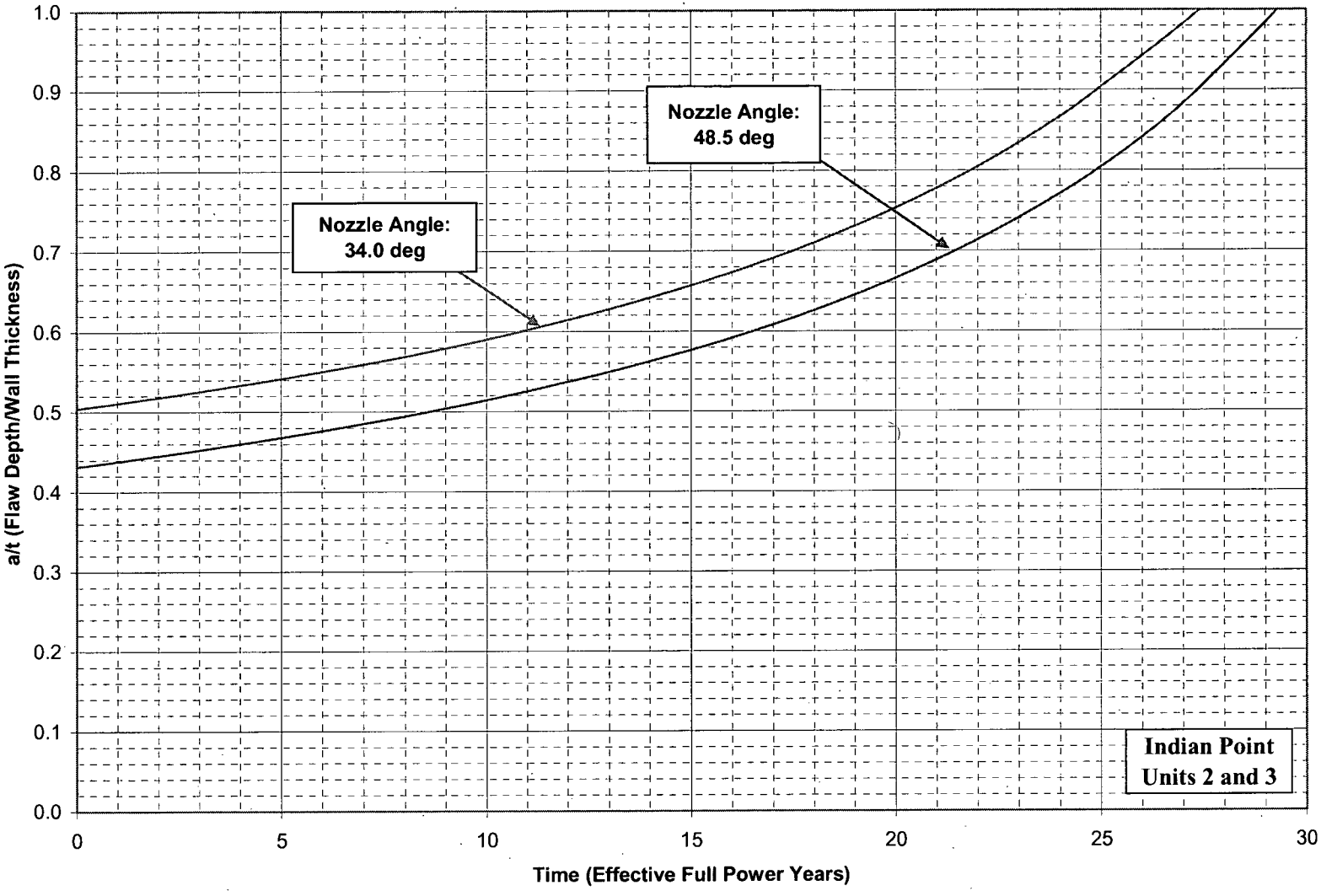

Figure 3-4 Crack Growth Results for Circumferential Outside Surface Flaws

3.5 Critical Flaw Size Determination

Critical Through-Wall Circumferential Flaw Length

Since circumferentially oriented flaws located below the J-groove weld of the BMI penetration nozzles may result in potential nozzle ejection, it is important to consider the possibility of crack extension in the circumferential direction. A series of crack growth calculations was performed for postulated through-wall circumferential flaws located just below the BMI penetration J-groove weld, in a plane parallel to the weld itself. This is the only flaw plane that could result in a complete separation of the BMI penetration nozzle. The objective of the calculation was to determine the maximum initial through-wall circumferential flaw length that would propagate around the circumference to a point where the remaining ligament of the penetration nozzle would reach plastic instability in less than 6 EFPY.

The critical circumferential through-wall flaw can be calculated by determining the required ligament which can conservatively withstand three times the design pressure acting on the nozzle bore and the crack face at flow stress levels in the ligament. The approach used is the same as that used for the upper head penetrations in EPRI MRP-44 EPRI report (Reference 8) as shown below:

[ ]

Using this approach, the critical circumferential through-wall half flaw angle (θ) calculated for the BMI penetration nozzle is 154°.

The results of crack growth calculation for through-wall circumferential flaws propagating around the circumference of the BMI penetration nozzles are shown in Figure 3-5. These crack growth curves begin at flaw lengths that result in stress intensity factors of 15 $MPa\sqrt{m}$ which exceeded the threshold value of 9 $MPa\sqrt{m}$. It should be noted that crack growths were conservatively calculated using the highest axial stress found along the plane parallel to the weld in the each of the BMI penetration nozzle. This is very conservative, since as discussed in Section 2.2, the actual axial stress at some circumferential locations is compressive and therefore cracks are not likely to propagate extensively in the circumferential direction. Figure 3-5 allows the determination of the maximum initial through-wall flaw length that would result in potential nozzle failure in 6 EFPY. As shown in Figure 3-5, the crack growth result for the outermost

penetration nozzle is more limiting and the required initial half through-wall flaw angle would be 104°, resulting in a total initial flaw length of 1.8 inch, which is well within the current NDE flaw detection capability. Since no indications were detected during the R17 outage, nozzle failure due to undetected circumferential flaw is not expected before the R20 outage.

Critical Through-wall Axial Flaw Length

Critical axial through-wall flaw length ($L_{critical}$) was calculated using the methodology provided in Section XI (Reference 9):

$$L_{critical} = 1.58\sqrt{Rt}\,[(\frac{\sigma_f}{(SF)\sigma_h})^2 - 1]^{1/2}$$

$$\sigma_h = PD_o/2t$$

Where:

P	=	pressure for loading condition
D_o	=	pipe outside diameter
R	=	mean pipe radius
t	=	wall thickness
S_y	=	yield strength
S_u	=	tensile strength
σ_f	=	flow stress $= (S_y + S_u)/2$
SF	=	safety factor

In order to be consistent with the methodology used in determining the critical flaw length required for circumferential flaws, the critical axial flaw length was conservatively calculated based on three times the design pressure by using a safety factor of 3.0. Using the above expression with a safety factor of 3.0, the critical through-wall axial flaw length calculated is 3.41 inch.

The results of crack growth calculation for through-wall axial flaws propagating along the length of the BMI penetration nozzles are shown in Figure 3-6. Note that crack growths were calculated using the hoop stress found along the length of nozzle on both the uphill and downhill sides of the nozzle. Figure 3-6 allows the determination of the maximum initial through-wall flaw length that would result in potential nozzle failure in 6 EFPY. As shown in Figure 3-6, the crack growth result for the outermost penetration nozzle is more limiting and the required initial flaw length is 0.8 inch, which is well within the current NDE flaw detection capability. Since no indications were detected during the R17 outage, nozzle failure due to undetected axial flaw is not expected before the R20 outage.

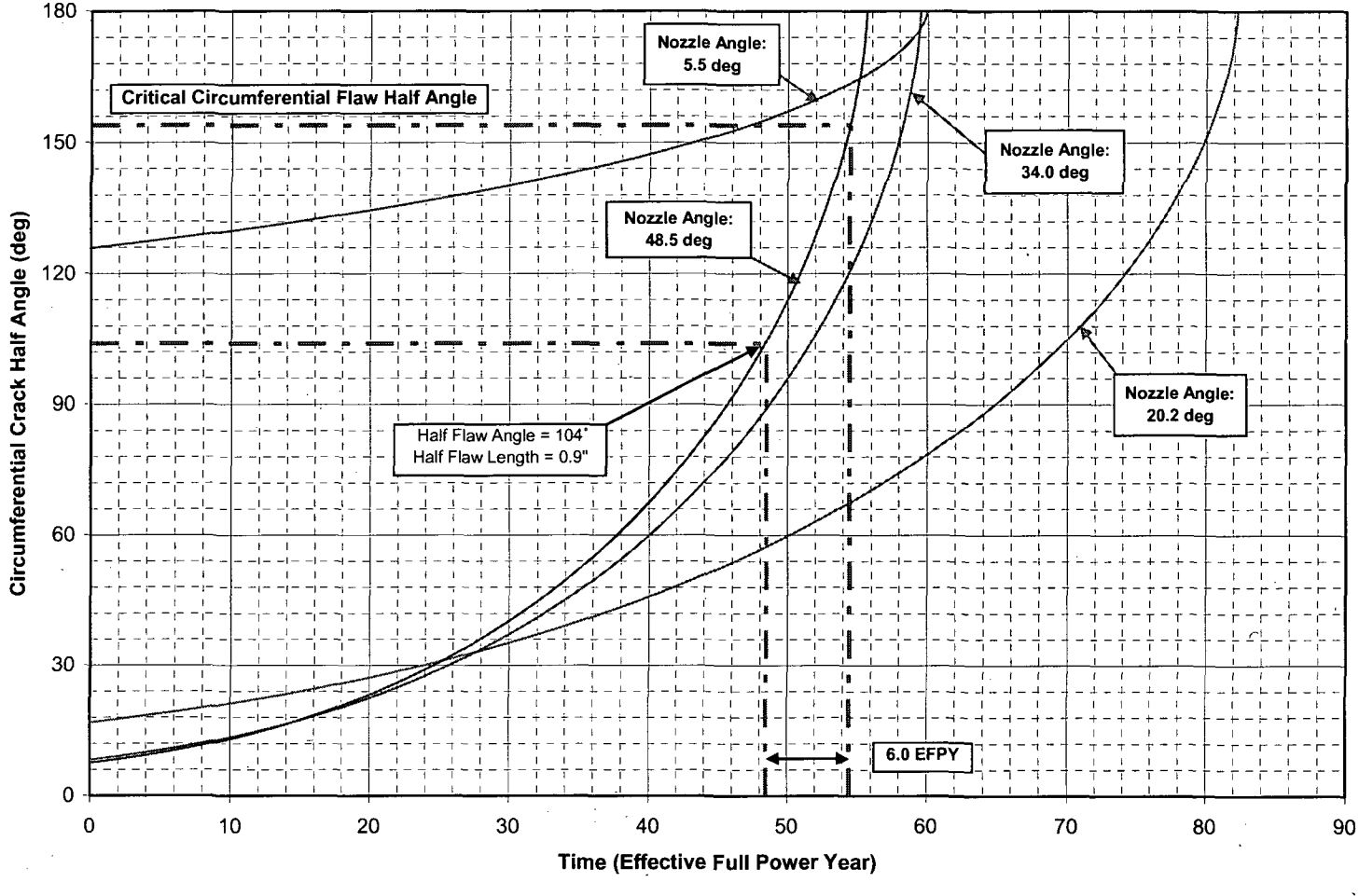

Figure 3-5 Crack Growth Results around the Circumference for Circumferential Through-wall Flaws

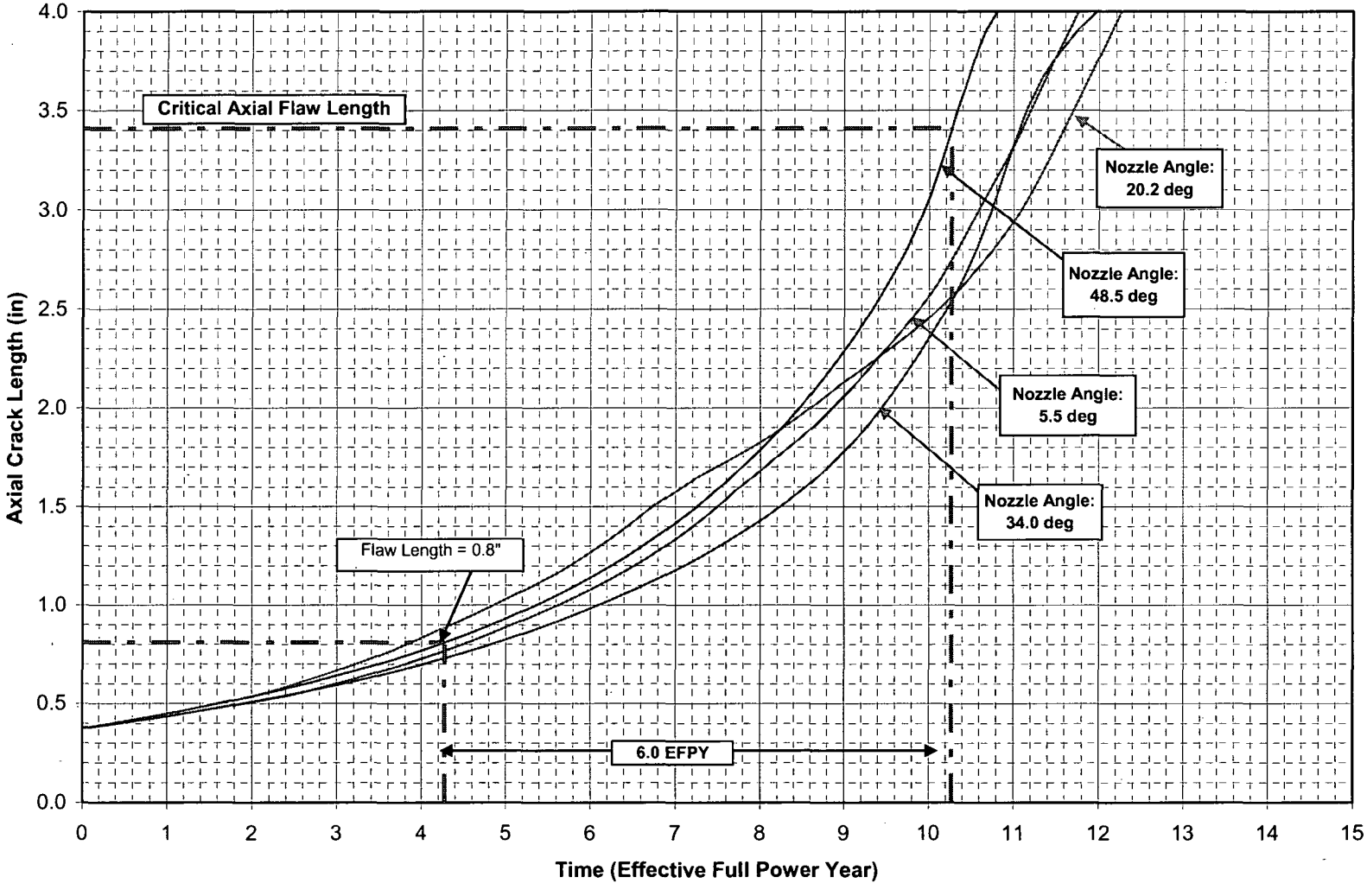

Figure 3-6 Crack Growth Results along the BMI Penetration Nozzle for Axial Through-wall Flaws

4.0 SUMMARY AND DISCUSSION

The purpose of this report is to provide a technical basis to support extension of the visual inspection surveillance interval of the BMI penetration nozzles at Indian Point Unit 2 to the R20 refueling outage in April of 2012. Since the BMI penetration nozzle configurations and geometries for both Indian Point Units 2 and 3 are quite similar, the results and conclusions provided in this letter report are also applicable to Indian Point Unit 3, if such technical basis is needed for Unit 3, provided the Unit 3 bottom head normal operating temperature is the same as Unit 2.

Finite element stress analyses were performed for the BMI penetration nozzles at Indian Point Units 2 and 3. Four BMI penetration nozzles for each unit were analyzed and the results were used to provide representative results for the remaining unanalyzed nozzles located on the reactor vessel bottom head. The bounding stress analysis results from both units were used as input to the structural integrity evaluation.

Structural integrity evaluation was performed to determine the time duration required for an undetected flaw in the BMI penetration nozzle to result in leakage, and the maximum initial flaw size that would result in potential nozzle failure before the R20 outage in April 2012.

The structural integrity evaluation consisted of crack growth analysis based on a conservative initial flaw size of 0.1 inch in depth and 0.6 inch in length. This assumed initial flaw size is larger than the maximum undetected flaw size ([ ] inch in depth and [ ] inch in length) based on the NDE detection capability during R17 outage for the BMI penetration nozzles. Both axial and circumferential flaws were considered in the crack growth evaluation. Based on the crack growth results shown in Figures 3-1 to 3-4, it can be concluded that axial outside surface flaw would provide the most limiting crack growth results. For an initial flaw depth of 0.10 inch and a flaw length of 0.60 inch, leakage is not expected to occur in less than 6 EFPY.

The maximum initial flaw size that would result in potential nozzle failure before the R20 outage in April 2012 was also determined as a part of the structural integrity evaluation. For circumferential through-wall flaw, the crack growth result for the outermost penetration nozzle is most limiting as shown in Figure 3-5, and the required initial flaw length is 1.8 inch. For axial through-wall flaw, the limiting required initial flaw length is 0.8 inch as shown in Figure 3-6 for the outermost penetration nozzle. These flaw lengths are well within the current NDE flaw detection capability. Since no indications were detected during the R17 outage, nozzle failure due to undetected axial or circumferential flaws is not expected before the R20 outage.

Field experiences indicate that any leakage from the BMI penetration nozzles is expected to be very low at least in the initial stages, and therefore not likely to result in any significant wastage of the reactor vessel bottom head. The boron acid deposits resulting from small leaks can be readily detected by visual examinations. For leakage approaching one gallon per minute, it is likely to be detected by current plant leakage monitoring system. In addition, the plant safety systems required to be operational during plant operation would be able to mitigate the effects of any significant leakage.

The results of the structural integrity evaluation, taking into consideration of the NDE detection capability, demonstrated that for any undetected flaws in the Indian Point Unit 2 BMI penetration nozzles, there are some margin of safety available pertaining to the occurrence of leakage and nozzle failure before the R20 outage in April 2012. Therefore, there would not be any safety concern pertaining to deferring the visual inspection to R20 outage in April 2012.

5.0 REFERENCES

1. Dominion Engineering Calculation No. C-8753-00-1 Revision 0, "Indian Point Unit 2 BMI Nozzle Stress Analysis."
2. Dominion Engineering Calculation No. C-8753-00-2 Revision 0, "Indian Point Unit 3 BMI Nozzle Stress Analysis."
3. Combustion Engineering Drawing E-232-056-5, "Instrumentation Penetration Assy. And Details – Bottom Head for Westinghouse Electric Corp 173" I.D. Reactor Vessel." (Westinghouse Proprietary Document)
4. Combustion Engineering Drawing E-234-056-4, "Instrumentation Penetration Assy. And Details – Bottom Head for Westinghouse Electric Corp 173" I.D. Reactor Vessel." (Westinghouse Proprietary Document)
5. WesDyne Memo dated 9/20/2007, "Flaw Detectability Assessment in Support of Indian Point 2 BMI Integrity Analysis." (Westinghouse Proprietary Document)
6. Materials Reliability Program (MRP) Crack Growth Rates for Evaluation Primary Water Stress Corrosion Cracking (PWSCC) of Thick-Wall Alloy 600 Material (MRP-55) Revision 1, EPRI, November 2002. (EPRI Proprietary Document)
7. Mettu, S. R., Raju, I. S., and Forman, R. G., NASA Lyndon B. Johnson Space Center report no. NASA-TM-111707, "Stress Intensity Factors for Part-through Surface Cracks in Hollow Cylinders," in Structures and Mechanics Division, July 1992.
8. PWR Materials Reliability Program, Interim Alloy 600 Safety Assessments for US PWR Plants (MRP-44): Part 2: Reactor Vessel Top Head Penetrations, EPRI, Palo Alto, CA: 2001. TP-1001491, Part 2. (EPRI Proprietary Document)
9. "Rules for In-Service Inspection of Nuclear Power Plant Component," ASME Code Section XI, 2001 Edition.

Appendix A

Flaw Detectability Assessment in Support of Indian Point Unit 2 BMI Integrity Analysis

WESDYNE INTERNATIONAL

P.O. Box 409
Madison, PA 15663
Bus. 724.722.5250
FAX 724.722.5830/5840

September 20, 2007

Subject: Flaw Detectability Assessment in Support of Indian Point 2 BMI Integrity Analysis

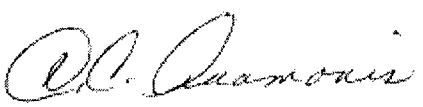

D.C. Adamonis, Vice President
Products and Applications Engineering

Cc: Fred Whytsell
Jack Lareau
Ed Shields
Conrad Wyffels